



Contents lists available at ScienceDirect

International Journal of Fatigue

journal homepage: www.elsevier.com/locate/ijfatigue

Equivalent stress concept to account for the effect of local cyclic stress ratio on transverse cracking in tension–tension fatigue

Vivek Richards Pakkam Gabriel^a, Mohamed Sahbi Loukil^b, Patrik Fernberg^{a,*}, Janis Varna^{a,c}

^a Department of Engineering Sciences and Mathematics, Luleå University of Technology, SE-97187 Luleå, Sweden

^b Department of Management and Engineering, Linköping University, SE-58183 Linköping, Sweden

^c Laboratory of Experimental Mechanics of Materials, Riga Technical University, LV-1048 Riga, Latvia

ARTICLE INFO

Keywords:

Polymer-matrix composites
Fatigue
Transverse cracking
Statistical methods

ABSTRACT

Presented test results on transverse cracking in cross-ply laminates upon tension–tension cyclic loading show that the increase of crack density depends not only on the maximum transverse stress in the cycle but also on the local cyclic stress ratio R_T^{loc} in the analyzed layer. To include the effect of the R_T^{loc} in the model with statistical failure stress distribution for crack initiation (based on Weibull distribution) adapted for fatigue, an equivalent stress is introduced in a similar manner as the equivalent strain energy release rate has been used for delamination crack propagation. The equivalent stress in the layer is defined as a power function of the maximum stress and the stress ratio in the layer. It was found, testing laminates with two different fiber contents that higher the local stress ratio in 90-layer, higher the transverse cracking resistance. Transverse crack density simulation using the developed equivalent stress model has been validated against test results.

1. Introduction

It is known that upon cyclic loading, damage in composite laminates evolves and eventually leads to catastrophic failure of the components [1]. Hence, it is important to predict life of polymer composites upon fatigue loading. Fatigue life can be defined as the number of cycles to disintegration of the laminate or to pre-determined level of allowed stiffness loss. In composite laminates, the first mode of damage is transverse cracking in off-axis layers with respect to the main tensile loading direction. These transverse cracks grow in both thickness direction and along the fibers to form tunnel like shape, unless they are stopped in low stress regions or by inhomogeneity in failure resistance (crack shielding etc.), see Fig. 1. In addition to that, transverse cracks increase in number when loaded continuously. Number of transverse cracks is most often represented in terms of transverse crack density (=number of cracks in a layer over unit length). Transverse crack density results in stiffness degradation of the composite laminate [2,3]. Methodology to determine stiffness degradation with respect to growth in crack density has been described in [4–6]. The current work presents a damage model developed to predict the crack density growth in tension–tension cyclic loading at arbitrary stress level and cyclic stress ratio in the layer.

In experiments, in the beginning, only one crack forms and more load/cycling is needed to create more cracks. The formation of an individual crack consists of 1) crack initiation and 2) crack propagation. **Crack initiation** starts at the edge with debonding of fiber and matrix followed by matrix cracking that coalesces with flaws to grow into a critical size in the thickness direction [2,7–9]. When the crack reaches a critical size, especially in a thick 90-layer as analyzed in this work, the energy release rate (ERR) is sufficient to instantly **propagate** the crack in both thickness and along the fiber direction [3,10–13]. In such case, the stress and the number of cycles required to initiate a crack to critical size becomes the failure resistance characteristics. The stress is the superposition of mechanical and thermal stress (stress caused by the difference between the curing temperature and test temperature) and can be calculated using the Classical Laminate Theory (CLT). Residual stress developed from the effect of shrinkage due to chemical reaction during manufacturing is not considered in the presented work. The failure resistance is different in different positions of the 90-layer, hence continuous increase in loading or the number of fatigue cycles is necessary to increase the number of cracks. The failure stress distribution in the 90-layer in quasi-static loading can be statistically defined using Weibull distribution [4,14,15].

In case of tension–tension cyclic loading at a given stress,

* Corresponding author.

E-mail address: patrik.fernberg@ltu.se (P. Fernberg).

<https://doi.org/10.1016/j.ijfatigue.2024.108482>

Received 8 April 2024; Received in revised form 27 June 2024; Accepted 28 June 2024

Available online 30 June 2024

0142-1123/© 2024 The Authors. Published by Elsevier Ltd. This is an open access article under the CC BY license (<http://creativecommons.org/licenses/by/4.0/>).

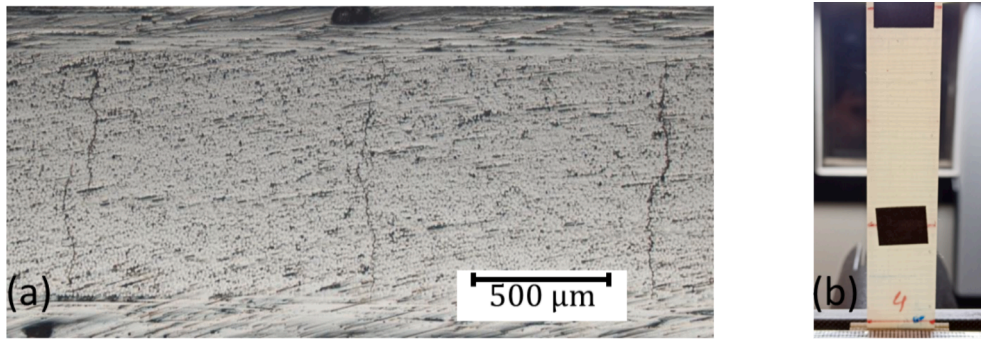


Fig. 1. Multiple cracks in 90-layer: a) Edge view b) Surface view, of GFEP [0/90₂]_s specimen.

propagation of cracks is governed by Paris law with respect to the ERR change within each cycle [16]. That is, a certain number of fatigue cycles are required to initiate a crack at a certain position and different number of cycles are required for the propagation of the cracks. However, from intermittent stop of fatigue experiments to characterize and quantify cracks, it was found that most of the cracks in this study were already tunnelling. This suggests that the number of additional cycles required for propagation was much smaller than the number needed for initiation. Hence, it is assumed that the number of cycles required for formation of transverse cracks across the entire specimen width is approximately equal to the number of cycles for initiation.

Based on this, the authors have developed Weibull-distribution based model, to predict the transverse crack density growth upon quasi-static tensile loading and tension–tension cyclic loading. In the developed model Monte-Carlo process is used to distribute failure properties and simulations are performed using Crack Opening Displacement (COD) based model for stress-distribution between cracks [5,6], predicting crack density growth both in non-interactive and interactive crack density region. The non-interactive crack density region is where the stress perturbations caused by two adjacent cracks are not interacting and do not affect the position of the next crack. Nevertheless, the model in [6] with parameters determined in tests at one fatigue stress level failed to predict crack density in test with different fatigue stress levels and cyclic stress ratio. Hence there is a necessity to revise the model. The current work addresses the changes in the fatigue model and accounts for the local stress ratio in the desired layer introducing an equivalent stress in the Weibull model.

From delamination tests it is known that R-ratio ($R = \sigma_{min}/\sigma_{max}$) affects the crack growth rate in the composites. Moreover, in fatigue delamination modeling, it was shown that neither the maximum strain energy release rate G_{max} nor $\Delta\sqrt{G}$, alone can give acceptable description to the R-ratio effect [17,18]. Hence in [19–23], the R-ratio effect (in terms of $\Delta\sqrt{G}$ or ΔK) was included along with K_{max} or G_{max} to predict delamination growth. Hojo et al [19,20], defined fatigue delamination growth model based on an empirical observation, that is

$$\frac{da}{dN} = CK_{eq}^n \quad (1)$$

and,

$$K_{eq} = K_{max}(1 - R)^{1-\gamma} \quad (2)$$

where, a is crack length, N is instantaneous number of cycles, K_{eq} is equivalent stress intensity factor similar to equivalent strain energy release rate and C and n are fitting parameters.

However, there are hardly any fatigue damage model developed for transverse crack initiation with the effect of the R-ratio. Likewise to delamination growth, the maximum stress in the cycle only or the stress range alone is not sufficient to characterize the effect of the fatigue cycle.

Inspired by (2), the equivalent stress concept is used in the current work to predict the density of initiated transverse cracks in fatigue. Similarly, as analyzing the process zone in delamination growth and assuming the same rules, authors visualize that during crack initiation (fatigue growth in through-the-thickness direction of a linked cluster of debonds), the localized high stress zone (K-zone) at the tip of the cluster degrades and eventually the cluster grows through this zone, becoming larger in the thickness direction. The growth rate depends on the maximum stress in the cycle and on the stress ratio in the layer. This “visualization” is the physical basis for the model presented below.

2. Theoretical aspects

2.1. Weibull failure stress distribution

Considering the layer as consisting of small elements in the transverse direction, the transverse stress required for crack initiation (called failure stress in following) in quasi-static loading is different in each element and Weibull distribution may be used to describe the variation. The two-parameter Weibull distribution (3) is defined by shape parameter m and scale parameter σ_0 . Determination of Weibull parameters is described in Section 4. Requirement that only one crack can be found in one element, leads to empirical conclusion that the element length cannot be larger than the 90-layer thickness [24].

In the used probability of failure P_f approach, the P_f of elements when the thermo-mechanical transverse stress in the layer changes from 0 to σ_T is equal to the number of broken elements,

$$P_f = \frac{\rho}{\rho_{max}} = 1 - \exp\left(-\left(\frac{\sigma_T}{\sigma_0}\right)^m\right) \quad (3)$$

where ρ is the crack density at stress σ_T and ρ_{max} is the maximum possible density when all elements (with length equal to ply thickness) are broken. In (3), σ_T is the transverse stress in the element.

At low crack density, the transverse stress σ_T averaged over ply thickness in many elements is similar to the CLT value for the 90-layer, $\sigma_T = \sigma_{T0}$. When the crack density increases, the stress perturbations from individual cracks start to overlap and transverse stress in the element depends on the distance to the neighboring crack. The averaged transverse stress at any positions between cracks is lower than the CLT value, $\sigma_T < \sigma_{T0}$ and it changes with introduction of new cracks. In this crack density region, Monte-Carlo simulation is a preferable tool, following, for example, the procedure described in [5,6].

In the Monte-Carlo process, a virtual specimen with 90-layer consisting of a very large number of elements along transverse direction of the fiber is created. A consequence of the assumption that cracks instantly grow in both thickness and along width direction once the applied stress in an element reaches or exceeds its failure stress, is that elements along thickness and width direction are not required and hence not created. The size of elements is selected based on same considerations as in previous studies: the element size should be small but not

smaller than the size of a typical fiber cluster consisting of at least 4–5 fibers [5]. Authors therefore assume that a typical fiber cluster size, and the element length, is 40 μm . Transverse failure stress of each element is assigned randomly distributing values from the Weibull distribution with experimentally determined Weibull parameters for the used material. The scale parameter σ_0^{MC} for small length elements (MC is a notation for Monte-Carlo simulations) is recalculated using the length ratio of element length in the reference test for Weibull parameter determination and the element length in Monte-Carlo simulation. In the Monte-Carlo procedure, the stress in elements between each pair of existing cracks must be calculated. Details regarding the stress distribution model developed by authors and used in this paper can be found in [5,6]. The simulation begins with introducing two cracks in end-elements of the virtual specimen. Then the thermo-mechanical transverse stress distribution between the introduced cracks is calculated by applying a unit stress. Thereafter, the failure index F_i ($= \frac{\text{applied stress}}{\text{failure stress}}$) for each element is determined. The element with highest F_i , is the element that fails next. Its position and the stress level when it happens is known. The crack is introduced in that element and stress between all pairs of cracks is calculated again finding an updated distribution of F_i . This procedure continues, until all elements are failed.

2.2. Assumptions regarding failure stress degradation in cyclic (fatigue) loading

Authors assume that the Weibull shape parameter m reflects the non-uniformity of fiber distribution in the 90-layer and, hence, it has the same value in quasi-static and in cyclic tests. In the suggested fatigue crack initiation scenario, the transverse failure stress in each position degrades during cyclic loading and the Weibull transverse failure stress distribution is changing. This overall reduction of the resistance of the ply to transverse failure during cyclic loading can be interpreted as a monotonous decrease of the scale parameter $\sigma_0^* = \sigma_0 f(N)$, where N is the number of cycles. Then, assuming a power law dependence of σ_0^* on the number of cycles, equation (3) can be rewritten as

$$\frac{\rho}{\rho_{max}} = 1 - \exp \left[- \left(\frac{\sigma_{T-max}^{fat}}{\sigma_0^*} \right)^m \right] = 1 - \exp \left[- N^n \left(\frac{\sigma_{T-max}^{fat}}{\sigma_0} \right)^m \right] \quad (4)$$

In (4) the stress state is represented by σ_{T-max}^{fat} – the maximum transverse stress in an element of the 90-layer during one cycle. n is the Weibull fatigue parameter. This description of fatigue effect on crack density has been used in [6,25].

2.3. Transverse stress ratio in 90-layer

In general, for layers with arbitrary off-axis angle the local ratios of different stress components, including shear, may vary. However, in axial loading of cross-ply laminates such as in the current paper and in [6], the damage is observed in 90-layer, hence effect of shear stress can be neglected.

In most studies like in [25–28], tension–tension cyclic testing was performed at several values of maximum laminate stress in the cycle and

constant load ratio, R . As expected, the crack density is higher when the maximum laminate stress in the cycle is higher. It should be noted that, even though the load ratio applied to the specimen is specified, the local thermo-mechanical transverse stress ratio in an individual layer is different and the local stress ratio R_T^{loc} (=minimum stress / maximum stress in 90-layer) change if the maximum laminate load is changed. This is due to residual thermal transverse stress caused by cool-down after manufacturing.

Previous studies using $R = 0.1$ [6] showed that at each macro-stress level the evolution of cracking can be described by Weibull distribution (4). However, an attempt to use Weibull parameters determined from test at one stress to predict cracking at a different stress using σ_{TO-max}^{fat} (=maximum fatigue stress in undamaged laminate) in Weibull model (4) failed. One of the reasons for failing could be the local transverse stress ratio R_T^{loc} that was also changing with changing the maximum applied load while keeping the R constant. In this paper, authors propose introducing a **local equivalent stress**, σ_{eq} , instead of σ_{TO-max}^{fat} in the Weibull model. The modified Weibull model is,

$$P_f = \frac{\rho}{\rho_{max}} = 1 - \exp \left[- N^n \left(\frac{\sigma_{eq}}{\sigma_0} \right)^m \right] \quad (5)$$

The equivalent stress in the layer is defined as

$$\sigma_{eq} = \sigma_{TO-max}^{fat} (1 - R_T^{loc})^\gamma, \quad (6)$$

This form is one of the investigated formulations that is simple and has least unknown parameters. The given definition of equivalent stress is inspired by work on delamination crack growth by Hojo et al. [19,20], and later also adopted by [29], where the stress ratio effect on Energy Release Rate (ERR) is introduced in a similar way. The applicability of this expression and determination of parameter γ is addressed in Section 5.

3. Materials and experimental methodology

Glass fiber reinforced epoxy, GFEP prepreg-based cross-ply laminates with two different layups and each with specific fiber content were manufactured using hot press. The two laminates [0/90]_s, and [0/90]₂_s had average thicknesses of 1.51 mm, and 1.36 mm and fiber content V_f of 38 %, and 58 % respectively. Thermo-elastic properties of layers in laminates were calculated using thermo-elastic properties of the fiber and resin applying micro-mechanics (RoM for longitudinal constants and Halpin-Tsai expressions for transverse and shear constants). The temperature difference ΔT between the manufacturing temperature and the room temperature is -95°C .

Coupon sized specimens were cut in dimensions of 200 mm x 15 mm from the manufactured laminates and reinforced with glass fiber epoxy tabs. The gauge length between the tabs was 100 mm. The edges were grinded and polished to minimize free edge effects and to facilitate optical microscopy observation of the damage state at edges.

Quasi-static tensile tests were performed at controlled displacement rate of 2 mm/min in INSTRON 3366 machine. The axial displacement was measured using extensometer within 50 mm gauge length. The specimens were loaded to predetermined strain level, to introduce damage to the specimens and then unloaded. After each step, the specimen was tested for stiffness degradation and the damage was quantified. To determine axial modulus, the specimen was loaded to strain level of 0.3 % and during the unloading ramp between 0.05–0.25 % strain, the modulus was measured. This stiffness measurement step does not introduce any new damage to the specimen. The cracks (that are covering the whole width of the specimen) were counted within the 50 mm gauge length of the specimen with aid of light source behind the specimen and the crack density was calculated. Then, the specimen was loaded to a predetermined strain level, larger than in the previous step to introduce more damage. This procedure was repeated until no more

Table 1
Cyclic test parameters and local stress ratio in 90-layer of each layup.

Layups and V_f (%)	Laminate strain % in first cycle	σ_{TO-max}^{fat} (MPa)	σ_{TO-min}^{fat} (MPa)	R_T^{loc}
[0/90] _s (38 %)	0.60	62.58	17.79	0.28
	0.50	54.28	16.96	0.31
	0.40	45.99	16.13	0.35
[0/90] ₂ _s (58 %)	0.40	66.37	17.31	0.26
	0.30	52.47	15.94	0.30

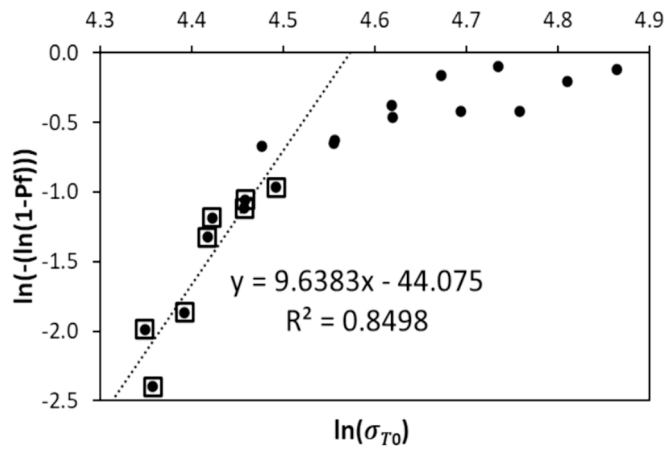


Fig. 2. Linear regression curve and fitting equation in static test performed on GFEP [0/90]s. Data points selected within $0.05 < P_f < 0.3$ are presented in black boxes.

increase in number of cracks was observed or specimen broken. The data were converted to crack density as a function of the thermo-mechanical transverse stress in 90-layer calculated using CLT.

Load controlled tension–tension cyclic tests were performed with frequency of 6 Hz and global load ratio $R = 0.1$ in the INSTRON E10000 Linear-Torsion machine. Cyclic tests were performed at different stress levels. In Table 1, for each laminate the strain corresponding to the first cycle, the maximum and minimum value of the local transverse stress in 90-layer of undamaged laminate during one cycle $\sigma_{T0_max}^{fat}$ and $\sigma_{T0_min}^{fat}$ (calculated using CLT) as well as the local stress ratio R_T^{loc} are shown.

Cyclic tests at selected load were performed in several intermittent steps, each next step with increasing number of cycles. After each step, axial modulus of the damaged specimen was measured, and cracks were counted using the same methodology as in quasi-static tests.

4. Data reduction

The procedure of parameter determination in the presented equivalent stress model for a given material consists of following steps: a) quasi-static tensile tests to gather crack density data for Weibull parameters m and σ_0 determination; b) cyclic loading tests, stopped after selected number of cycles N , are performed at selected reference combination of $\sigma_{T0_max}^{fat}$, R_T^{loc} to find parameter n that characterizes the dependence on the number of cycles; c) test data for different combinations of $\sigma_{T0_max}^{fat}$ and R_T^{loc} are fitted using the above parameter values and the equivalent stress σ_{eq} as a fitting parameter in (5); d) the obtained σ_{eq} dependence on $\sigma_{T0_max}^{fat}$ and R_T^{loc} is fitted with (6), obtaining parameter γ . Steps a) and b) are described in this section.

Table 2

Weibull parameters for 90-layer in laminates with different fiber content.

Layups	Shape parameter m	Scale parameter σ_0 (MPa)	Fatigue parameter n
[0/90]s	9.64	96.83	0.71
[0/90 ₂]s	4.86	127.22	0.77

4.1. Quasi-static testing for m and σ_0 determination

The Weibull parameter determination in static tensile loading was in detail explained in [5,6]. As an example, the m and σ_0 parameter determination for 90-layer in GFEP [0/90]s laminate is shown below. Assuming that the crack density is low, transverse stress between cracks can be approximated as the thermo-mechanical transverse stress in the layer from CLT, $\sigma_T = \sigma_{T0}$, from (3) follows

$$\ln\left(-\ln\left(1 - \frac{\rho}{\rho_{max}}\right)\right) = m \ln \sigma_{T0} + m \ln \sigma_0 \tag{7}$$

The Weibull parameters are determined within the range of $0.05 < P_f < 0.3$, that in case of [0/90]s laminate is $0.12 < \rho < 0.42$ cr/mm. According to (7) the Weibull shape m and scale σ_0 parameter can be determined applying linear fit to data in Fig. 2, obtaining $m = 9.64$ and $\sigma_0 = 96.83$ MPa.

4.2. Tension-tension cyclic testing: n determination

In cyclic loading, Weibull fatigue parameter n in (4) can be determined by transforming (4) to ln-ln axis,

$$\ln\left(-\ln\left(1 - \frac{\rho}{\rho_{max}}\right)\right) = n \ln N + m \ln \frac{\sigma_{eq}}{\sigma_0} \tag{8}$$

According to equation (8), n is the slope of $\ln\left(-\ln\left(1 - \frac{\rho}{\rho_{max}}\right)\right)$ versus $\ln N$ data and for this purpose at this stage the definition of σ_{eq} (as in (6)) is irrelevant. For GFEP [0/90]s this test was conducted at $\sigma_{T0_max}^{fat} = 54.28$ MPa (0.5 % laminate strain in first cycle, see Table 1). Weibull fatigue parameter, n , was determined using data points in the interval 0.07 cr/mm $< \rho < 0.41$ cr/mm that corresponds to the P_f range in [5,6] which is $0.05 < P_f < 0.3$. From the linear fitting expression in Fig. 3(a), which has the same form as (8), the parameter for [0/90]s is $n = 0.71$. Value of n for [0/90₂]s is the slope given in Fig. 3(b).

5. Results and discussions

5.1. Experimental data

One of the conditions for development of effective fatigue model is a minimized number of physical tests required for parameter determination. Thus, the Weibull shape parameter m and the scale parameter σ_0

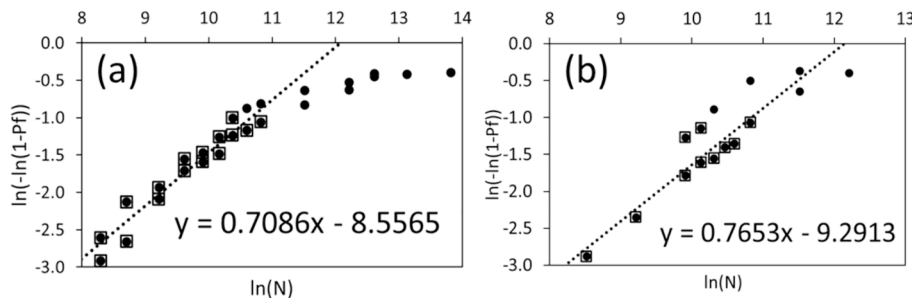


Fig. 3. Linear regression curve of the fatigue test data and fitting equation: a) [0/90]s at $\sigma_{T0_max}^{fat} = 54.28$ MPa; b) [0/90₂]s at $\sigma_{T0_max}^{fat} = 52.47$ MPa in the 90-layer. Data points selected within $0.05 < P_f < 0.3$ are presented in black boxes.

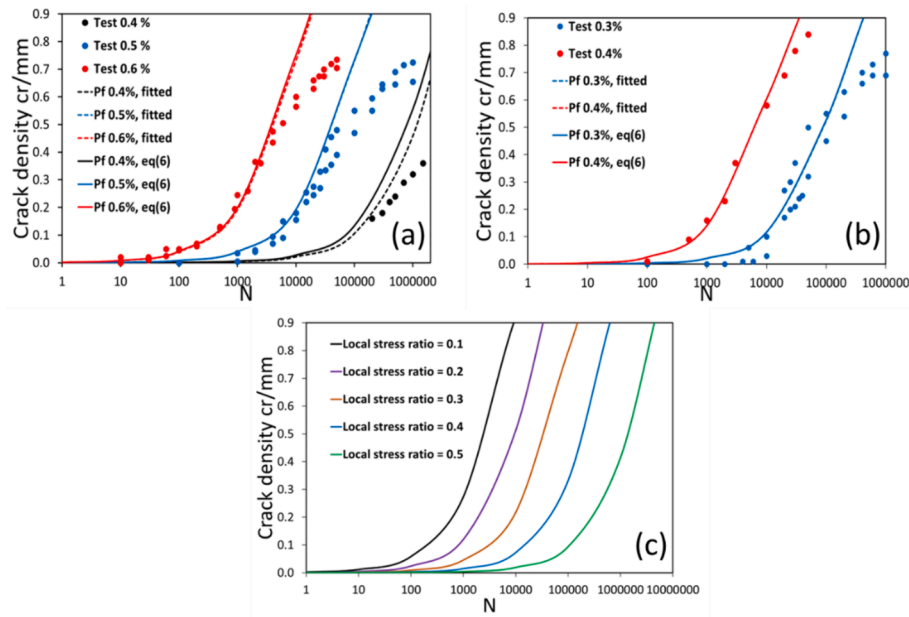


Fig. 4. Crack density in cyclic load in a) [0/90]s laminate; b) [0/90₂]s; c) Effect of the local stress ratio according to P_f model in [0/90]s laminate. Dots are experimental data points, dashed and solid lines are P_f based predictions (predictions using fitted σ_{eq} and using (6) respectively).

for each composite were defined in a quasi-static test, measuring crack density growth with the applied strain. The parameters for two different laminates, presented in Table 2, depend on fiber content in the 90-layer. It appears that the shape parameter is decreasing with increasing fiber content. However, this conclusion may be erroneous because the laminate with higher fiber content had thicker 90-layer that may be more crucial for variability of fiber clusters. In our assumptions, the nonuniform fiber distribution defines the value of the shape parameter. No distinct trend can be seen in Table 2 for the scale parameter dependence on ply thickness and/or fiber content. Increasing scale parameter with decreasing 90-layer thickness, which is typical for very thin plies in laminates (as observed in [30]), was not observed, maybe, because the 90-layer in the [0/90]s laminate is rather thick (0.72 mm) and the fiber content is low leading to low transverse modulus.

Cyclic tests at 0.3 % maximum strain in first cycle were used to determine the fatigue parameter n for 90-layer in [0/90₂]s, see Fig. 3(b) and 0.5 % maximum strain for [0/90]s. Values for the two laminates are given in Table 2.

Crack density growth with number of cycles in [0/90]s specimens tested at three different stress levels, see Table 1, is shown in Fig. 4(a) (colored dots are test results). As expected, the crack density at a given number of cycles is higher when stress level in 90-layer is higher. Similar trends may be observed in Fig. 4(b) for [0/90₂]s laminate. Crack density growth starts to slow down with increase in number of cycles. That could be because a) cracks are forming in interactive region, where the stress between cracks is lower than the far field stress in the layer; b) only the “strongest” positions in the layer are not broken yet. Also, growth of delaminations from the crack tips at the interface between 0- and 90-layer and fiber breakages in 0-layer near the crack tips were

witnessed, additionally reducing the stress between cracks.

5.2. Equivalent stress determination using P_f based simulations

The distribution parameters obtained for each laminate at one stress level were used to predict crack density growth at different stress levels, using (4) and utilizing the assumption that the transverse stress in any position is equal to the CLT stress, $\sigma_T = \sigma_{T0}$ (P_f approach that is valid in the region where the neighboring cracks are not interacting with each other, that is in the low crack density region). Hence, the predicted results from the P_f –approach are expected to be in a good agreement with test results in the low crack density region only.

As shown in Table 1, even for the same laminate at fixed applied R , the local stress ratio, R_T^{loc} changes dependent on the applied load due to presence of residual thermal stresses.

Since the effect of the R_T^{loc} on cracking was not known, the first attempt was to ignore its effect and make predictions using the maximum stress in the cycle as the equivalent stress, $\sigma_{eq} = \sigma_{T0,max}^{fat}$. This attempt failed dramatically without showing any trend in discrepancy.

To gain more information regarding proper definition of the equivalent stress, simulations were performed using σ_{eq} as a fitting parameter in the P_f expression (5). For convenience, the σ_{eq} values determined by data fitting and the corresponding lines are referred as “fitted” in Fig. 4 (a) and (b) and in text. The fitted equivalent stress values for each fatigue stress level in both layouts are given in Table 3.

Then, the fitted equivalent stress values given in Table 3 were used to find calculated equivalent stress by fitting a constant γ in (6) for each laminate. γ is different for different laminates because of significant

Table 3

Fitted equivalent stress σ_{eq} , γ and calculated equivalent stress (6) for all tested layouts and loading cases.

Layups	Laminate strain % at first cycle	$\sigma_{T0,max}^{fat}$ (MPa)	R_T^{loc}	Fitted σ_{eq} (MPa)	γ	Calculated equivalent stress (6) (MPa)
[0/90]s	0.60	62.58	0.28	48.00	0.78	48.21
	0.50	54.28	0.31	40.50		40.53
	0.40	45.99	0.35	32.00		32.84
[0/90 ₂]s	0.40	66.37	0.26	28.50	2.80	28.48
	0.30	52.47	0.30	19.00		19.03

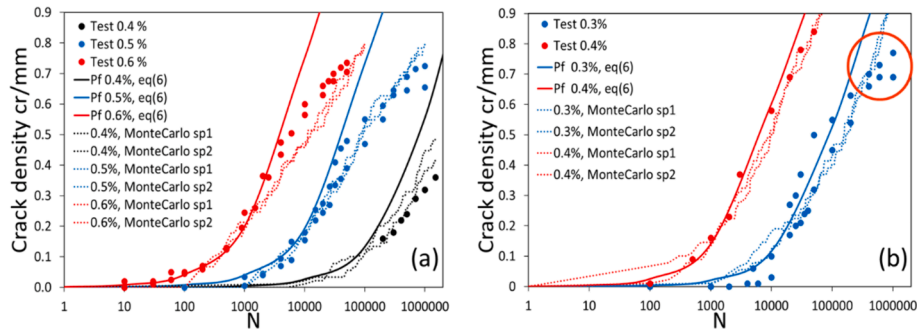


Fig. 5. Simulation and test results for specimens from a) [0/90]s; b) [0/90]2s; Dotted lines are two Monte-Carlo simulations of a given test.

differences in fiber content. Results shows that γ is larger for composites with higher fiber content (laminate [0/90]2s).

Parametric analysis using the identified model as in (5) and (6) showing the effect of local stress ratio in the damaged layer, is shown in Fig. 4(c). Simulations were made using $\sigma_{TO_max}^{fat} = 54.28\text{MPa}$, $\gamma = 0.78$ and $R_T^{loc} = 0.1$ to 0.5 in steps of 0.1, in (6). It can be seen that keeping the same maximum stress in 90-layer and changing the local stress ratio, the crack density growth changes significantly. Crack density prediction using the equivalent stress from (6) is given in Fig. 4(a). The difference between using the best fit values and (6) is small. Similar conclusions were obtained analyzing cracking in GFEP [0/90]2s specimens, presented in Fig. 4(b).

Thus, the equivalent stress model (6) in (5), was validated for GFEP specimens with two different layups and fiber volume fractions. However, cyclic tests need to be performed in different material systems to inspect the generality of the proposed equivalent stress based Weibull model for crack initiation in fatigue. To minimize the experimental work, an optimized methodology is to be developed to determine the equivalent stress parameters.

5.3. Cracking simulation in cyclic loading by Monte-Carlo method

It can be observed in Fig. 4 that predictions of the P_f – approach are in good agreement with data in the non-interactive crack density region only. At high crack density, the P_f approach that assumes that stress between cracks is the same as in CLT over-predicts the stress and consequently also the crack density. Thus, a model capable to capture stress distribution between each pair of cracks must be used along with the Monte-Carlo method to predict cracking in the high crack density region. The simulation procedure is described in Section 2.1.

Using the Weibull parameters and the equivalent stress according to (6) for the respective layups and stress levels, the crack density growth as a function of the number of fatigue cycles has been simulated with the use of Monte-Carlo method and stress distribution model. In Fig. 5, the two dotted curves for each loading case are predictions using two Monte-Carlo process realizations (two virtual specimens with randomly allocated Weibull failure stress in elements are created). For all stress levels in [0/90]s, and [0/90]2s laminates, the predicted crack density is in good agreement with the test results. However in [0/90]2s, especially in cyclic test at $\sigma_{TO_max}^{fat} = 52.47\text{MPa}$ (0.3 % laminate strain at first cycle), the predicted crack density in the high density region is higher than the experimental, marked with red circle in Fig. 5(b). At that stage, the crack density growth in the test almost stopped. A possible reason is the growth of delamination between 0 and 90-layer starting from the transverse crack tips and fiber breakages in 0-layer near the crack tips. The delamination and fiber breakages additionally reduces the stress between cracks and forming another crack between them is difficult. Since the employed stress distribution model doesn't account for delaminations, the predicted stress is too high and it leads to over-predicted crack density. Hence, the current stress distribution model is

not suitable for accurate Monte-Carlo simulations when large delaminations are present. Normalized axial modulus reduction data presented in Appendix confirm these conclusions. At higher fatigue cycles, the axial modulus of the laminate becomes lower than the axial modulus of the static tested laminate.

6. Conclusions

The concept of Weibull transverse failure stress distribution in the 90-layer was used to analyze evolution of transverse cracking in tension–tension cyclic loading of cross-ply laminates with relatively thick 90-layer where initiated cracks almost instantly propagated as tunnels along the fiber direction. Data analysis showed that the crack density dependence on thermo-mechanical transverse stress in the layer cannot be described by a model employing the maximum value of the transverse stress in the cycle only. Introducing equivalent transverse stress that depends on the maximum stress in the cycle and also on the local thermo-mechanical stress ratio R_T^{loc} in the ply, the description of transverse cracking is much better, as evidenced by experimental data for two GF/EP composite cross-ply laminates with different 90-layer thickness and with rather different fiber content. The R_T^{loc} effect on the equivalent stress is described by a power function and methodology is presented for parameter determination in the equivalent stress expression. The approach is used in Monte-Carlo simulations to describe cracking in high crack density region where stress state between existing cracks is calculated after each cracking event. The approach is validated in the limited number of tests and proven to be an efficient tool to predict transverse crack density growth in tension–tension cyclic loading for laminates with relatively thick plies.

CRedit authorship contribution statement

Vivek Richards Pakkam Gabriel: Writing – original draft, Visualization, Validation, Methodology, Investigation, Formal analysis, Data curation. **Mohamed Sahbi Loukil:** Writing – review & editing, Supervision. **Patrik Fernberg:** Writing – review & editing, Supervision, Resources, Project administration, Methodology, Funding acquisition. **Janis Varna:** Writing – original draft, Supervision, Methodology, Investigation, Funding acquisition, Formal analysis, Conceptualization.

Declaration of competing interest

The authors declare that they have no known competing financial interests or personal relationships that could have appeared to influence the work reported in this paper.

Data availability

Data will be made available on request.

Acknowledgements

Work done in the presented paper are funded by Swedish

Aeronautical Research Program NFFP 7 [project number 2019-02777] & 8 [project number 2023-01199] and GKN Aerospace, Sweden.

Appendix A

Laminate axial modulus degradation

Axial modulus degradation due to increase of crack density in the 90-layer was measured in quasi-static tensile tests as well as in cyclic loading tests at different load levels and local stress ratio R_T^{loc} in the damaged layer. In Fig. A1 the normalized axial modulus of the laminate $E_{xn} = E_x^{LAM}/E_{x0}^{LAM}$ is shown for two layups, where E_x^{LAM} and E_{x0}^{LAM} are axial modulus of damaged and undamaged laminates respectively. In both layups shown in Fig. A1, data points from tensile static tests and cyclic tests are showing the same trends and dependence in low crack density region. That means that the appearance of the cracks and their COD is similar in both types of loading. However, in the high crack density region, modulus reduction is higher in cyclic loaded specimens. The most probable reason is delamination growth from the crack tips and fiber breakage in the adjacent 0-layer near the crack tips.

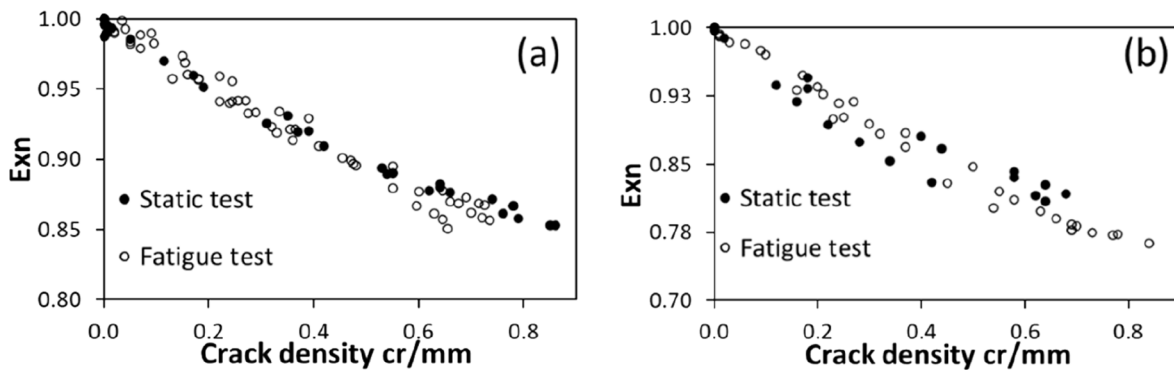


Fig. A1. Normalized axial modulus 'Exn' degradation versus crack density growth in a) [0/90]s b) [0/90]2s laminates.

References

- Jamison RD, Schulte K, Reifsnider KL, Stinchcomb WW. Characterization and analysis of damage mechanisms in tension-tension fatigue of graphite/epoxy laminates, Effects of defects in composite materials. ASTM STP 836, American Society for Testing and Materials 1984;21-55.
- Paris F, Cano J, Varna J. The fiber-matrix interface crack – a numerical analysis using boundary elements. Int J Fracture 1990;82(1):11–29. <https://doi.org/10.1007/BF00017861>.
- Parvizi A, Bailey JE. On multiple transverse cracking in glass fiber epoxy cross-ply laminates. J Mater Science 1978;13(10):2131–6. <https://doi.org/10.1007/BF00541666>.
- Varna J. Modeling mechanical performance of damaged laminates. J Compos Mater 2013;47(20–21):2443–74. <https://doi.org/10.1177/0021998312469241>.
- Pakkam Gabriel VR, Loukil MS, Varna J. Analysis of intralaminar cracking in 90-ply of GF/EP laminates with distributed ply strength. J Compos Mater 2021;55(26):3925–42. <https://doi.org/10.1177/00219983211027346>.
- Pakkam Gabriel VR, Loukil MS, Varna J. Intralaminar cracking during cyclic loading in laminates with distributed failure stress in 90-ply. Int J Fatigue 2022; 161:106909. <https://doi.org/10.1016/j.ijfatigue.2022.106909>.
- Zhuang L, Pupurs A, Varna J, Talreja R, Ayadi Z. Effects of inter-fiber spacing on fiber-matrix debond crack growth in unidirectional composites under transverse loading. Compos A 2018;109:463–71. <https://doi.org/10.1016/j.compositesa.2018.03.031>.
- Zhuang L, Talreja R and Varna J. Transverse crack formation in unidirectional composites by linking of fibre/matrix debond cracks. Composites: Part A 2018;107: 294–303. DOI: 10.1016/j.compositesa.2018.01.013.
- Herráez M, Mora D, Naya F, Lopes CS, González C, Llorca J. Transverse cracking of cross-ply laminates: a computational micromechanics perspective. Compos Sci Technol 2015;110:196–204. <https://doi.org/10.1016/j.compscitech.2015.02.008>.
- Paris F, Blazquez A, McCartney LN, Mantic V. Characterization and evolution of matrix and interface related damage in [0/90]s laminates under tension, Part I: Numerical predictions. Compos Sci Technol 2010;70:1168–75. <https://doi.org/10.1016/j.compscitech.2010.03.004>.
- Nairn JA. Matrix microcracking in composites. In: Kelly A, Zweben C, Talreja R, Manson J-A, editors. Comprehensive Composite Materials: Polymer Matrix Composite. Amsterdam: Elsevier; 2000. p. 403–32.
- Parvizi A, Garrett KW, Bailey JE. Constrained cracking glass fiber-reinforced epoxy cross-ply laminates. J Mater Sci 1978;12:195–201. <https://doi.org/10.1007/BF00739291>.
- Bailey JE, Parvizi A. On the fiber debonding effects and the mechanism of transverse-ply failure in cross-ply laminates of glass fiber/thermoset composites. J Mater Sci 1981;16(3):649–59. <https://doi.org/10.1007/BF02402782>.
- Peters PWM. The strength distribution of 90° plies in 0/90/0 Graphite-Epoxy laminates. J Compos Mater 1984;18(6):545–56. <https://doi.org/10.1177/002199838401800604>.
- Manders PW, Chou TW, Jones FR, Rock JW. Statistical analysis of multiple fracture in 0°/90°/0° glass fiber/epoxy resin laminates. J Mater Sci 1983;18:2876–89. <https://doi.org/10.1007/BF00700768>.
- Quaresimin M, Carraro PA, Mikkelsen LP, Lucato N, Vivian L, Brøndsted P, et al. Damage evolution under cyclic multiaxial stress state: A comparative analysis between glass/epoxy laminates and tubes. Compos Part B: Eng 2014;61:282–90. <https://doi.org/10.1016/j.compositesb.2014.01.056>.
- Rans CD, Alderliesten R, Benedictus R. Misinterpreting the results: how similitude can improve our understanding of fatigue delamination growth. Compos Sci Technol 2011;71:230–8. <https://doi.org/10.1016/j.compscitech.2010.11.010>.
- Khan R. Delamination growth in Composites under fatigue. TU Delft Netherland; 2013 [Ph.D. thesis].
- Hojo M, Tanaka K, Gustafson CG, Hayashi R. Effect of stress ratio on near-threshold propagation of delamination fatigue cracks in unidirectional CFRP. Compos Sci Technol 1987;29(4):273–92. [https://doi.org/10.1016/0266-3538\(87\)90076-5](https://doi.org/10.1016/0266-3538(87)90076-5).
- Hojo M, Ochiai S, Gustafson CG, Tanaka K. Effect of matrix resin on delamination fatigue crack growth in CFRP laminates. Eng Fract Mech 1994;49(1):35–47. [https://doi.org/10.1016/0013-7944\(94\)90109-0](https://doi.org/10.1016/0013-7944(94)90109-0).
- Atodaria DR, Putatunda SK, Mallick PK. A fatigue crack growth model for random fiber composites. J Compos Mater 1997;31(18):1838–55. <https://doi.org/10.1177/002199839703101804>.
- Atodaria DR, Putatunda SK, Mallick PK. Delamination growth behavior of a fabric reinforced laminated composite under mode I fatigue. J Eng Mater Technol 1999; 121(3):381–5. <https://doi.org/10.1115/1.2812390>.
- Atodaria DR, Putatunda SK, Mallick PK. Fatigue crack growth model and mechanism of a random fiber SMC composite. Polymer Compos 1999;20(2):240–9. <https://doi.org/10.1002/pc.10351>.
- Reifsnider KL, Jamison R. Fracture of fatigue-loaded composite laminates. Int J Fatigue 1982;4(4):187–97. [https://doi.org/10.1016/0142-1123\(82\)90001-9](https://doi.org/10.1016/0142-1123(82)90001-9).
- Carraro PA, Maragoni L, Quaresimin M. Prediction of the crack density evolution in multidirectional laminates under fatigue loadings. Compos Sci Technol 2017;145: 24–39. <https://doi.org/10.1016/j.compscitech.2017.03.013>.
- Maragoni L, Carraro PA, Peron M, Quaresimin M. Fatigue behaviour of glass/epoxy laminates in the presence of voids. Int J Fatigue 2017;95:18–28. <https://doi.org/10.1016/j.ijfatigue.2016.10.004>.

- [27] Hoang NT, Gamby D, Lafarie-Frenot MC. Predicting fatigue transverse crack growth in cross-ply carbon-epoxy laminates from quasi-static strength tests by using iso-damage curves 2010;32(1):166-173. DOI: 10.1016/j.ijfatigue.2009.02.045.
- [28] Mohammadi B, Rohanifar M, Davood S-M, Farrokhabadi A. Micromechanical prediction of damage due to transverse ply cracking under fatigue loading in composite laminates. J Reinforced Plast Compos 2017;36(5):377–95. <https://doi.org/10.1177/0731684416676635>.
- [29] Hosoi A, Kawada H. Fatigue life prediction for transverse crack initiation of CFRP cross-ply and quasi-isotropic laminates. Materials 2018;11(7):1182. <https://doi.org/10.1177/0731684416676635>.
- [30] Pupurs A, Loukil MS, Marklund E, Varna J, Mattsson D. Transverse crack initiation in thin-ply laminates subjected to tensile loading at low and cryogenic temperatures. Mechanics Compos Mater 2024;59:1049–64. <https://doi.org/10.1007/s11029-023-10156-0>.